



**HAL**  
open science

## Determination of the mechanical properties of gelatinized starch granule from bulk suspension characterization

Arnesh Palanisamy, Gabrielle Moulin, Marco Ramaioli, Artemio Plana-Fattori, Denis Flick, Paul Menut

► **To cite this version:**

Arnesh Palanisamy, Gabrielle Moulin, Marco Ramaioli, Artemio Plana-Fattori, Denis Flick, et al.. Determination of the mechanical properties of gelatinized starch granule from bulk suspension characterization. *Rheologica Acta*, 2022, 10.1007/s00397-022-01325-4 . hal-03626461

**HAL Id: hal-03626461**

**<https://hal.science/hal-03626461>**

Submitted on 31 Mar 2022

**HAL** is a multi-disciplinary open access archive for the deposit and dissemination of scientific research documents, whether they are published or not. The documents may come from teaching and research institutions in France or abroad, or from public or private research centers.

L'archive ouverte pluridisciplinaire **HAL**, est destinée au dépôt et à la diffusion de documents scientifiques de niveau recherche, publiés ou non, émanant des établissements d'enseignement et de recherche français ou étrangers, des laboratoires publics ou privés.

# Determination of the mechanical properties of gelatinized starch granule from bulk suspension characterization

Arnesh Palanisamy<sup>a</sup>, Gabrielle Moulin<sup>a</sup>, Marco Ramaioli<sup>a</sup>, Artemio Plana-Fattori<sup>a</sup>, Denis Flick<sup>a</sup>, Paul Menu<sup>t</sup><sup>a,\*</sup>

<sup>a</sup>*Université Paris Saclay, INRAE, AgroParisTech, UMR SayFood, 91300, Massy, France*

---

## Abstract

Gelatinized starch granules are soft and deformable particles that are commonly used in food products as texture modifiers. Modelling the flow behaviour of such suspensions during industrial processes requires the knowledge of the mechanical properties of the swollen granules, however, such data is usually lacking because of the difficulties inherent to the determination of mechanical properties of particles that are heterogeneous in terms of size and shape. We investigate here the rheological properties of dense suspensions prepared at different volume fractions and by different means (centrifugation, limited water swelling, osmotic compression) to estimate the mechanical properties of an "averaged" starch granule. Results show that starch granule exhibits a rough surface and behave as frictional particles. We compare the shear modulus value determined assuming either frictionless (previous model) or frictional interactions (as suggested by our results), the latter giving shear modulus lower by about one order of magnitude. This study also allows the first estimate of the starch granule bulk modulus, which value is corresponding to a Poisson ratio of 0.47, close to the maximum value of 0.5. The swollen granule shear modulus is also shown to be temperature independent in the range commonly found in industrial processes (20-90 °C). These results pave the way towards multiscale mechanistic modelling of the flow of starch suspensions, to derive macroscopic rheological properties from the description of the microscopic granule properties.

*Keywords:* Microgel, Shear modulus, Bulk modulus, Thermal effects, Particle Elasticity

---

## 1. Introduction

In its native form, starch is found as dense granules in a variety of grains and tubers. After industrial fractionation and in some cases, chemical/thermal treatments, a large variety of starch granules with contrasted properties are obtained. These starch granules that differ in terms of textural properties, or stability against mechanical, Physico-chemical or thermal stresses, are produced for various specific applications such as enhanced oil recovery in oil drilling applications or thickening agents in food products (Ratnayake and Jackson, 2008; Nawaz et al., 2020). Global starch production is expected to reach around 156 metric tonnes by 2025 (Reportlinker.com, 2020), of this roughly 60% is used for food-based applications and 40% is expected to be used for industrial uses including oil, pharmaceutical, paper, etc.

Thermal treatments are commonly used in food processing and are usually applied to products that are highly hydrated. Applying a thermal treatment to native starch granules in the presence of excess water results in important modifications of their properties. In their native state, starch granules are solid particles, more or less spherical, in which starch macromolecules (amylopectin and amylose) are densely packed so that these granules only have a very limited water absorption capacity. However, if the temperature exceeded  $\sim 70^\circ\text{C}$ , an important swelling of the particles is very rapidly observed if water is available around the granule. The influx of water is driven by the enthalpic interactions between the hydrogen bonding sites of starch and water (Renzetti et al., 2021). This process, during which the particle can absorb more than 10 times its mass in water, is called gelatinization. During gelatinization, the volume fraction of the starch particles present in a starch suspension strongly increases, and so does the suspension viscosity.

If the volume fraction of the particles in solution remains very low, i.e. much below the random close packing volume fraction  $\phi_{rcp}$ , that is the maximum volume fraction that can be reached by solid undeformable particles packed randomly, it behaves as a hard particle suspension at low shear rates (Einstein, 1905; Batchelor, 1977). However, at high enough starch volume fractions, these suspensions form thick pastes (gelatinization is also called

---

\*corresponding author

*Email address:* paul.menut@agroparistech.fr (Paul Menut)

28 starch pasting(Chen et al., 2007)) which exhibit properties that are similar to the ones  
29 of dense suspensions of soft microgel particles, with both solid-like and fluid-like proper-  
30 ties(Seth et al., 2006). At low stresses, they behave like elastic solids and deform reversibly  
31 under stress. However, once sufficient stress is reached they begin to flow and show the  
32 properties of a fluid. The threshold stress at which they begin to flow is called the yield  
33 point. Soft particle pastes have a jammed amorphous microstructure that is the source of  
34 their rheological behaviour. At volume fractions higher than  $\phi_{rcp}$ , soft particles start to  
35 deform to accommodate more neighbouring particles (Menut et al., 2012; de Aguiar et al.,  
36 2018). Further compression results in particle shrinkage. Therefore, their volume fraction,  
37 also called packing fraction, that is estimated from the volume occupied by the particles in  
38 the diluted state, can exceed 1 (Seth et al., 2006; Evans and Lips, 1992).

39 With the advent of particle-based simulation methods, such as Discrete Element Mod-  
40 elling and CFD-DEM, there is significant interest in developing simple methods to charac-  
41 terize material properties such as particle Young’s modulus and Poisson’s ratio, required as  
42 a model input. One of the most common contact models used for simulating particles is  
43 the Hertzian contact model. This model takes into account the curvature of the spherical  
44 surfaces while predicting the interaction forces on the colliding particles. According to this  
45 contact model, a repulsive force exists when the granules overlap and no force exists when  
46 they do not overlap (Di Renzo and Di Maio, 2005). To predict these normal and tangential  
47 repulsive forces one needs two parameters namely, Young’s modulus and Poisson’s ratio.  
48 To fully describe suspensions behaviour, lubrication forces need to be integrated, they arise  
49 due to the presence of the fluid layers in between particles. The momentum of a granule  
50 is imparted to the surrounding fluid and subsequently the other granules, hence leading to  
51 transport of momentum, even when granules are not physically in contact with each other.  
52 One requires interstitial fluid viscosity, surface roughness, position and velocities of particles  
53 for predicting the lubrication forces. For homogeneous isotropic materials, simple relations  
54 exist between the three elastic constants are Young’s modulus, the bulk modulus and the  
55 shear modulus. These relations allow calculating them all as long as two are known, as they  
56 are related by the following equations.

$$K = \frac{E}{3(1 - 2\nu)} \quad (1)$$

$$G = \frac{E}{2(1 + \nu)} \quad (2)$$

57 where  $K$ ,  $G$ ,  $E$  and  $\nu$  are respectively the bulk modulus, shear modulus, Young’s mod-  
 58 ulus and Poisson’s ratio. These relations could be applied to describe the whole behaviour  
 59 of dense suspensions, which at a macroscopic scale could be considered homogeneous and  
 60 isotropic. Individual starch granules, however, are non-spherical particles, and their in-  
 61 dividual behaviour might deviate significantly from one of the homogeneous and isotropic  
 62 particles. Therefore a strategy could be to determine only “averaged” properties, as it is usu-  
 63 ally done for example for their size determination, done by static light scattering assuming  
 64 a spherical shape.

65 Techniques at the particle level exists for deciphering materials properties of individ-  
 66 ual particle material properties in literature (Villone et al., 2019; Villone and Stone, 2020;  
 67 Abate et al., 2012; Mohapatra et al., 2017). Typical techniques include atomic force mi-  
 68 croscopy(AFM) based on nano-indentation, Brillouin light scattering(BLS), microfluidics,  
 69 tensionmeter. In AFM based techniques a Poisson ratio is assumed and the Young’s modulus  
 70 is deducted from resisting force vs displacement data (Kaufman et al., 2017; Aufderhorst-  
 71 Roberts et al., 2018). However, these techniques are not straightforward to apply to measure  
 72 a particle averaged modulus for such a complex system of soft particles with a very high  
 73 degree of variability in terms of size and shapes. BLS data is used to infer the Poisson’s  
 74 ratio (Mohapatra et al., 2017). In microfluidic approaches, a particle is compressed through  
 75 a tapered channel and as pressure is developed by increasing the flow rate, the particle de-  
 76 forms due to the pressure and penetrates further into the channel. The penetration depth  
 77 is optically observed and Young’s modulus is deduced (Villone et al., 2019). Similarly, ten-  
 78 siometer and microgel based techniques make use of surface tension to generate force for  
 79 deformation and optical techniques for measuring the deformation (Abate et al., 2012; Vil-  
 80 lone and Stone, 2020). However, the applicability of these techniques is not straightforward

81 for non-spherical, poly-disperse, complex suspensions such as starch suspensions. Typical  
82 DEM models make the spherical particle assumption, albeit the ‘multi-sphere’ approach and  
83 methods for specific shapes such as super-quadratics exists (Lane et al., 2010; Preece et al.,  
84 1999). For non-spherical particles with no particular shape features, it is a standard practice  
85 to simulate spherical particles with averaged particle properties. One simple methodology to  
86 obtain such average particle properties is to infer them from the bulk response of the dense  
87 suspensions, which behave macroscopically as homogeneous isotropic materials, and then to  
88 determine from that an ”averaged” properties at the level of the individual particles. Such  
89 use of average ‘calibration techniques’ are also a common feature in powder and dry granu-  
90 lar material simulations using DEM (He et al., 2015; Yan et al., 2016; Orefice and Khinast,  
91 2020). This approach is also useful in ‘coarse-graining’ simulations where the actual system  
92 is too large and one simulates at a mesoscale with larger ‘representative particles’ instead of  
93 actual particle sizes to reduce the computational costs.

94 In this article, the average mechanical properties of a large population of starch granules  
95 are investigated from bulk rheological measurements conducted on dense suspensions. To  
96 estimate the average particle shear modulus, the suspension shear modulus was measured  
97 . Two extreme hypothesis were considered, namely the fully frictional and the friction-less  
98 scenarios, to determine an upper and a lower limit for the particle shear modulus. The  
99 likelihood of the two assumptions is critically discussed. Then, we investigate the particles  
100 bulk modulus by osmotic compression. Finally, we investigate how particles shear modulus  
101 depend on the temperature, in the range 20-90°C.

## 102 **2. Materials and methods**

103 Chemically cross-linked waxy maize starch (C\*Tex 06205), provided by Cargil (Bauppte,  
104 France) was used for the entire study. Waxy maize starch contains more than 99 % amy-  
105 lopectin, and chemical cross-linking prevents the release of macromolecules during gelatiniza-  
106 tion.

107 *2.1. True density measurement*

108 The starch particles true density was measured using an air pycnometer (micromeritics  
109 AccuPyc 1330). We determined a true density  $\rho_{true, starch} = 1.321 \pm 0.002$  g/ml (average  
110 value from 6 repeats).

111 *2.2. Centrifugation*

112 In a 2-litre mixing vessel, we introduced 15 grams of starch before the addition of 1 litre  
113 of distilled water. The mixture was heated to 90 °C while mixing a 50 rpm using an IKA  
114 eurostar 60 mixer with a 3 blade propeller of diameter 5 cm; and held at this temperature for  
115 15 minutes to ensure complete swelling of the starch granules. After letting the suspension  
116 cool down to room temperature, it was transferred into centrifuge tubes and centrifuged  
117 (SIGMA 3-18KS centrifuge) in the required conditions of rotation speed and duration. The  
118 supernatant (excess water layer) was carefully removed and the pellet, which consisted of  
119 densely packed swollen starch granules, was recovered for rheological characterization and  
120 dry weight measurements to estimate the volume fraction. A combination of centrifugation  
121 speeds ranging from 500g to 10000g and centrifugation duration ranging from 15 minutes  
122 to 30 minutes resulted in swollen starch suspensions with volume fractions  $\phi$  ranging from  
123 0.447 to 0.552.

124 *2.3. Osmotic compression*

125 22.5 grams of starch were added to 1.5 l of distilled water in a mixing vessel. The mixture  
126 was gelatinized at 90 °C as described previously (2.2). After letting the suspension cool  
127 down to room temperature, it was transferred into a regenerated cellulose dialysis tube with  
128 a cut-off of 6-8 kDa (spectra/por 1, diameter 40 mm). The dialysis tube was clipped at both  
129 ends and placed for osmotic compression inside a solution of Poly-Ethylene Glycol (PEG,  
130  $20\text{kg}\cdot\text{mol}^{-1}$ ) of known concentration. After osmotic compression, the compressed samples  
131 were recovered and subjected to rheological characterization and dry weight measurements  
132 to estimate their volume fraction. We used PEG 20kDa concentrations ranging from 0.2%  
133 to 5% (wt/wt) and compression times ranging from 2 to 15 days to produce samples with  
134 volume fractions  $\phi$  ranging from 0.46 to 1.69.

135 For the estimation of bulk modulus, we used the same protocol as described above,  
136 however, to ensure a constant osmotic pressure (that could decrease with time due to water  
137 diffusion from the sample to the PEG bath), the PEG bath was renewed 3 times. To  
138 determine the osmotic pressure corresponding to a given PEG concentration, we used the  
139 phenomenological one-parameter equation of state proposed by Cohen et al. (2009), which  
140 correctly described the behaviour of PEG (and others neutral flexible polymers in good  
141 solvents). This equation, based on the sum of a van 't Hoff and a des Cloizeaux terms, include  
142 a fitted parameter  $\alpha$ , also called the “crossover index”, which is polymer size-dependent and  
143 for which we used the value proposed by Li et al. (2015) for PEG 20kDa. In that case, the  
144 osmotic compression lasted around 17 days to ensure equilibrium without any degradation  
145 or granule softening.

#### 146 *2.4. Limited water swelling*

147 After the addition of a known quantity of starch (ranging from 5 to 25 grams) into  
148 100ml of water in a mixing vessel, the suspension was heated up to 90 °C and held at this  
149 temperature for 15 min under constant mixing. The sample was then cooled down to room  
150 temperature and recovered for rheological characterization and dry weight measurements.  
151 This resulted in starch suspension with volume fractions  $\phi$  ranging from 0.42 to 1.90.

#### 152 *2.5. Dry weight measurement and volume fraction determination*

153 Dry weight measurements were conducted at 100 °C in an oven (Chopin technologies).  
154 Prior measurements showed that after 24h at 100 °C the sample had reached a constant  
155 weight, therefore all samples were let in the oven for 24h before dry weight measurement.  
156 Samples were introduced in an aluminium foil previously weighted, and the weight of the  
157 sample was determined before ( $M_1$ ) and after ( $M_2$ ) drying so that the sample dry starch  
158 content could be determined as  $S_{dry} = M_2/M_1$ . Therefore, the starch concentration in the  
159 suspension,  $C_s$  (in g of starch per 100g of water) is given by  $C_s = 100 * \frac{S_{dry}}{1-S_{dry}}$



160 The corresponding equivalent volume fraction of unswollen starch granules,  $\phi_{ug}$ , is given by

$$\phi_{ug} = \frac{C_s}{\rho_{true,starch}} * \frac{1}{100 + \frac{C_s}{\rho_{true,starch}}} \quad (3)$$

161 With  $\rho_{true,starch}$  the true density of unswollen starch previously determined assuming density  
162 for water  $\rho_{water} = 1000 \text{ kg/m}^3$ .

163 To estimate the volume fraction of swollen granules, we used data from previous micro-  
164 scopic experiments showing that, on average, the starch granule radius (the geometric mean  
165 of the Feret diameters) increases 2.35 times when gelatinized in excess of water (Palanisamy  
166 et al., 2020; Deslandes et al., 2019). Thus, assuming that the granules are spherical and the  
167 total volume is conserved (volume gained by the starch during swelling is lost by water),  
168 one can estimate the volume of the swollen starch granules divided by the volume of the  
169 suspension:  $\phi$ , which is also known as the volume fraction. Please note that based on the  
170 definition here volume fraction is notional and thus can exceed 1. Similar definitions have  
171 been used extensively in the literature for various other suspensions as well (Mattsson et al.,  
172 2009).

$$\phi = (2.35^3) * \phi_{ug} \quad (4)$$

## 173 2.6. Rheology

174 The rheological measurements were all performed in a Couette cell using an Anton Paar  
175 MCR92 rheometer. The characterization of the dense suspensions of swollen starch granules  
176 was performed at 20 °C. The mechanical properties were first probed at constant frequency  
177 ( $f = 1 \text{ Hz}$ ) and strain ( $\gamma = 0.01$ ) for 120 seconds, with an acquisition rate of 1 point per  
178 second. Then, a frequency sweep was carried out at constant strain  $\gamma = 0.01$ , from  $f = 0.02$   
179 Hz to  $f = 3.5 \text{ Hz}$ . Storage modulus obtained from single point measurements are plotted in  
180 figure 1. The frequency and loading effects were negligible compared to the volume effects.

181 The effect of temperature on the rheological properties was also evaluated. A rejuve-  
182 nation and ageing step was performed prior to the first measurement, in order to limit

183 measurements error resulting from the sample history ( Cloitre et al. (2000)). Rejuvenation  
184 consists of shearing the sample at shear stress greater than the yield stress thus allowing  
185 the flow of the sample. Here, the sample was sheared at a shear rate  $\dot{\gamma} = 50 \text{ s}^{-1}$ . The  
186 following ageing step consists in holding the sample at rest for 45 minutes. Sedimentation  
187 experiments showed the absence of settling in the sample during all the duration of the  
188 experiments, which can be attributed to the large volume fraction of the samples (above  
189 random loose packing), combined with a low density difference between the swollen starch  
190 granules and the surrounding water. Rheological properties were measured at 20 °C; 40 °C,  
191 60 °C, 80 °C and finally 90 °C, the ramp rate during heating being 2 °C per minute. At  
192 each temperature, the rheological properties were measured at constant frequency  $f = 1 \text{ Hz}$   
193 and constant strain  $\gamma = 0.01$  for 120 seconds with an acquisition rate of 1 point per second.  
194 For cooling the sample from 90 °C to 20 °C, a ramp rate of 0.4 °C per minute was used, and  
195 sample properties were again measured once thermal equilibrium was reached.

## 196 *2.7. Confocal laser scanning microscopy*

197 Gelatinized samples obtained by the limited water swelling method and characterized  
198 by a particle volume fraction close to 0.4 were observed using a confocal laser scanning  
199 microscope (CLSM) (Leica TCS SP8, Germany). 0.5 ml of starch solution was stained using  
200 50  $\mu\text{L}$  of Congo Red solution (1% in water, Sigma-Aldrich). Two 250  $\mu\text{m}$  thick spacers were  
201 used to place the stained solutions on the microscope slides. The solutions were excited  
202 with a laser at 488 nm and the emitted fluorescence was detected in the range 497 - 717 nm.  
203 The laser was used at 85% of the maximum intensity. Samples were observed with a 40X  
204 water objective. The total number of pixels in each picture is 3224 x 3224 and each pixel  
205 correspond to 0.09  $\mu\text{m}$ . Thus, the length and width of each picture corresponds to 290.62  
206  $\mu\text{m}$ . A total of 192 scans were performed using 0.422  $\mu\text{m}$  step for a total sample height of  
207 80.67  $\mu\text{m}$  to generate a stack of images. Each of these 192 images was manually analyzed  
208 to count the number of neighbours of some representative granules.

209 *2.8. Bulk modulus measurements through osmotic compression*

210 To measure the bulk modulus of the suspension using osmotic compression, one first needs  
 211 to establish the time taken for the sample to equilibrate osmotically with the surrounding  
 212 medium. To do so, we followed the dry weight evolution during osmotic compression, at two  
 213 different PEG concentrations, and determined the corresponding volume fraction (Table 1).  
 214 After 17 days, the volume fraction tend to reach a plateau. Above 17 days, the increase  
 215 in volume fraction is very limited, but we observed by rheology a decrease in the sample  
 216 shear modulus, that could result from starch degradation and granule softening, thus only  
 217 samples obtained after 17 days will be considered for analysis.

time [days]	$\phi$ -3% PEG20K [wt/wt]	$\phi$ -4% PEG20K [wt/wt]
4	0.76	0.99
9	1.20	1.60
14	1.39	1.67
17	1.45	1.69
21	1.46	1.75
24	1.47	1.75

Table 1: Evolution of the sample volume fraction during osmotic compression, at two different PEG concentrations

218 **3. Results and Discussion**

219 *3.1. Suspension rheology and estimation of the particle shear modulus*

220 We observed that starting from  $\phi \sim 0.4$ , suspensions exhibit a finite value of elastic mod-  
 221 ulus. By contrast to what is observed in colloidal systems, which are liquid till the random  
 222 closed packing, suspensions of granular particles can exhibit a finite modulus at volumes  
 223 fractions much lower, due to the formation of a self-supporting stress-bearing network. The  
 224 minimum volume fraction at which this network can form is called the random loose packing,  
 225 its value depends on the shape but also the frictional properties of the particles(Silbert, 2010;  
 226 Dong et al., 2006). Starting from the random loose packing, the shear modulus (measured  
 227 at  $f = 1\text{Hz}$  and  $\gamma = 0.01$ ) of dense suspensions of swollen starch granules strongly increases  
 228 with volume fraction, as illustrated in figure 1. Whatever the method used to prepare dense

229 suspensions, namely centrifugation, osmotic compression or limited water swelling, the data  
 230 superimposed. Whatever the history associated with each procedure, the final stage that  
 231 is reached is reproducible in terms of rheological characterization and the granule volume  
 232 fraction is the key parameter that controls the elastic behaviour of the paste. Even in the  
 233 case of limited water swelling, for which granule never reached their full swelling capacity  
 234 due to the limited amount of water (for  $\phi > 1$ ), the properties of the suspension are identical  
 235 to the one of fully swollen starch granules that were partially dehydrated by compression.  
 236 Two regimes are observed concerning the elastic modulus dependency toward volume frac-  
 237 tion. First, from above the random loose packing to  $\phi \approx 0.7$ , the shear modulus strongly  
 238 increases with the volume fraction. Then, a transition zone exists for  $0.7 < \phi < 1$ . For  
 239 volume fraction  $\phi > 1$ , the dependence of shear modulus on volume fraction is much weaker.  
 240 Insert in Figure 1 shows the log-log plot which shows the existence of the two regimes and  
 241 the power law dependence of shear modulus with the notional volume fraction of granules.  
 242 Fitting a power law to these regimes resulted in the following equation

$$G' = \begin{cases} 1600\phi^{3.15} & 0.4 \leq \phi \leq 0.7 \\ 550\phi^{0.53} & 1 \leq \phi \end{cases}$$

243 A similar increase in shear modulus with notional volume fraction have been reported  
 244 by Evans and Lips (1990); Abdulmola et al. (1996); Rodriguez-Hernandez et al. (2006). The  
 245 existence of two regimes of shear modulus with volume fraction for swollen starch suspensions  
 246 is reported in Evans and Lips (1992). Also, for comparison Evans and Lips (1992) reported  
 247 values of suspension shear modulus around 750 Pa and 1000 Pa at notional volume fraction  
 248 of 1, for two different grades of chemically modified maize starches.

249 Whatever the volume fraction, the elastic modulus of the suspension only show a very  
 250 weak dependency on the frequency. This is illustrated in the insert of figure 1 for 3 different  
 251 volume fractions achieved via 3 sample preparation methods, in the first, intermediate and  
 252 second regime. As reported by Seth et al. (2006), soft particle suspension moduli are function  
 253 of the frequency. Seth et al. (2006) even predicted from simulations  $G_0$  and  $G_\infty$  (storage

254 moduli at low and high frequency). We show from the following data that the relationship  
 255 of storage moduli with frequency are similar across the volume fractions tested.

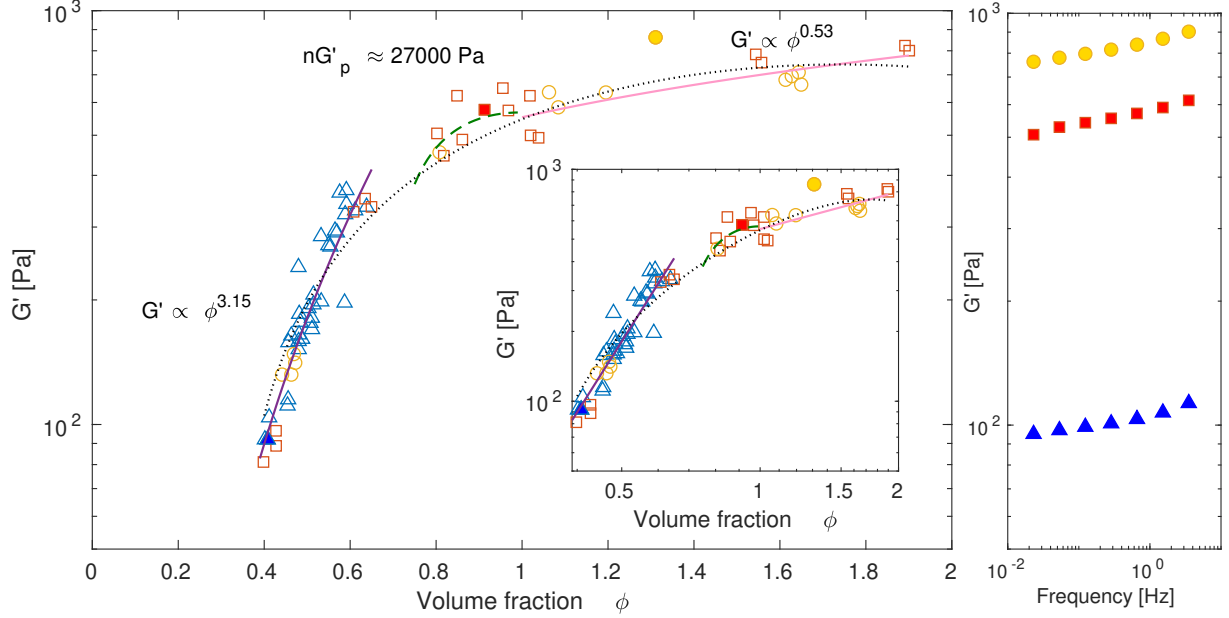


Figure 1: Suspension shear modulus as a function of volume fraction. Triangles[ $\Delta$ ], Squares[ $\square$ ], circles[ $\circ$ ] represent samples prepared via centrifugation, limited water swelling and osmotic compression respectively ( $\gamma = 0.01$ ,  $f = 1$  Hz). The solid dotted line represents the polynomial fit of overall experimental data ( $G_{suspension} = -352\phi^2 + 1229\phi - 330$ ). The purple continuous line represents the power-law fit for volume fractions  $\phi < \phi_{rcp}$ , Green dashed line represents the best fit from the Evans and Lips (1990) model for  $0.8 < \phi < 1$ , Pink continuous line represents the power law fit for volume fractions  $\phi > 1$ . *Insert*: The same figure in the log-log plot.

*Right-side plot*: Dependence on frequency: volume fraction of three samples prepared via centrifugation, limited water swelling and osmotic compression correspond to 0.4, 0.91, 1.31.

256 For friction-less systems, Evans and Lips (1990) derived an analytical equation that links  
 257 the suspension shear modulus with the individual granule shear modulus and the average  
 258 number of neighbouring granules. This model assumes a Hertzian potential (contact model)  
 259 between granules. The equation, valid for  $\phi_{rcp} < \phi < 1$ , is as follows:

$$G'_{susp} = \frac{\phi_{rcp} n G'_p}{5\pi(1-\nu)} \left( \left( \frac{\phi}{\phi_{rcp}} \right)^{\frac{1}{3}} \left( 1 - \left( \frac{\phi}{\phi_{rcp}} \right)^{-\frac{1}{3}} \right)^{\frac{1}{2}} - \frac{8}{3} \left( \frac{\phi}{\phi_{rcp}} \right)^{\frac{2}{3}} \left( 1 - \left( \frac{\phi}{\phi_{rcp}} \right)^{-\frac{1}{3}} \right)^{\frac{3}{2}} \right) \quad (5)$$

260 where  $G'_{susp}$  is the suspension shear modulus,  $\phi_{rcp}$  is the volume fraction at random close

261 packing and  $n$  is the average number of neighbouring granules respectively.

262 Given a granule size distribution one can estimate the  $\phi_{rcp}$  based on the relationship  
263 proposed by Farr and Groot (2009) as previously done in Shewan and Stokes (2015a,b);  
264 Shewan et al. (2021). In the system investigated, the size distribution of Feret diameters  
265 of swollen starch granules has been previously determined, it is characterized by a normal  
266 distribution with mean =  $33.1 \mu\text{m}$  and standard deviation =  $10.7 \mu\text{m}$ . With this value,  $\phi_{rcp} =$   
267  $0.68$  was determined. The average number of neighbours for each granule,  $n$ , was estimated  
268 using confocal microscopy. This method was previously used for PMMA spheres by van der  
269 Vaart et al. (2013) and also allowed to measure the pair correlation function. In fact, they  
270 predicted suspension shear moduli at high frequency with Young's modulus obtained from  
271 atomic force microscopy and pair correlation function from confocal microscopy.

272 In figure 1 we show the fit of equation 5 for the truncated data in the volume fraction  
273 range of  $\phi_{rcp} < \phi < 1$ . As we can see from equation 5,  $G_p$  depends on the assumption of  
274 the average coordination number  $n$  of each granule. To determine  $n$ , confocal images were  
275 acquired on suspensions and the coordination number of 10 different granules was manually  
276 counted for each of them, based on the contacts that were observed in different layers.

277 Figure 2 shows the confocal cross-section image of the starch granule suspension at  
278  $\phi = 0.4$ , the maximum fraction that could be reached for which each granule could still be  
279 easily distinguished from its neighbours. Here,  $\phi < \phi_{rcp}$  and  $n$  could depend on  $\phi$  (van  
280 Hecke, 2009), the value determined at this volume fraction might differ from the one at  
281  $\phi = 1$ , that should be used to apply the Evans and Lips model. Experimental studies have  
282 shown that once particles are in contact, further compression first result in a decrease in the  
283 void fraction de Aguiar et al. (2018) and local deformation at the contact point de Aguiar  
284 et al. (2017). As a result, the increase in coordination number with volume fraction might be  
285 limited, especially if friction is present in the system. From the image acquired by confocal  
286 microscopy, it is evident that the starch granules are far from being spherical. It should be  
287 noted that if the granule seems hollow, this is likely due to the fact that dye (congo red) is  
288 adsorbed only on the surface of the granule. In figure 2 we tracked one selected granule from  
289 its base (top-left image) to its top (bottom-right image). For this selected granule 5 contacts

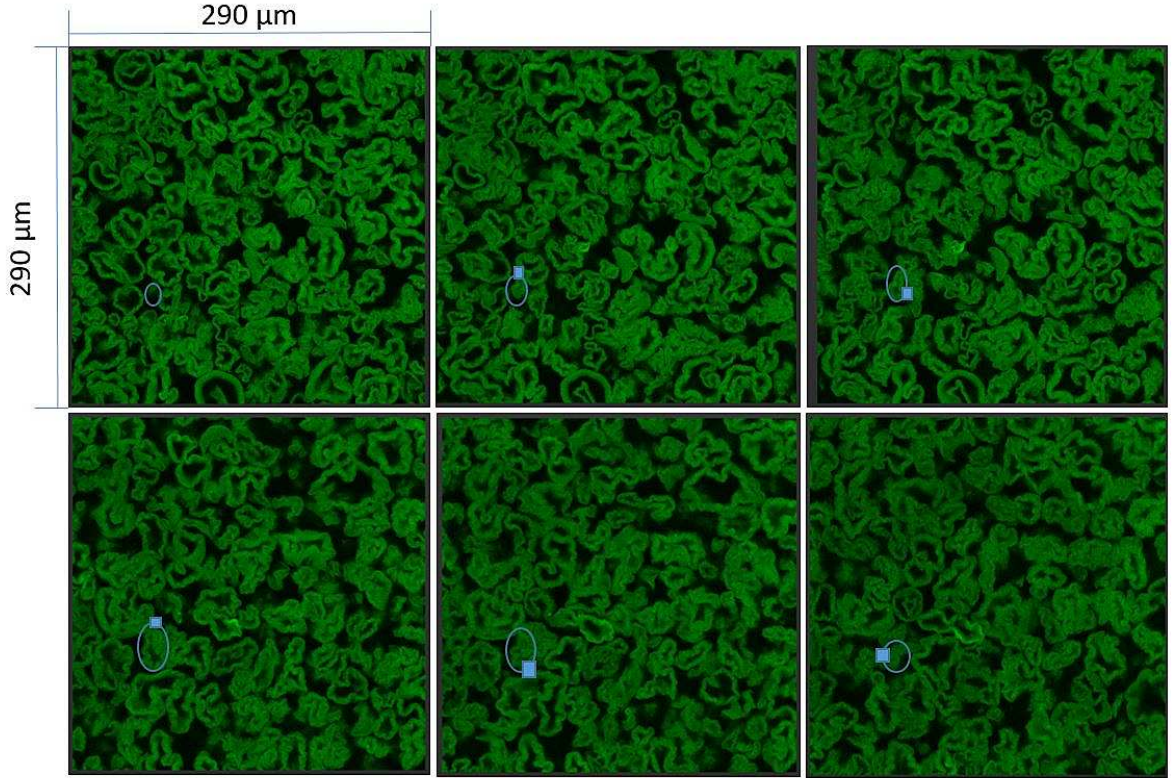


Figure 2: Confocal stack images of starch granule suspension.  
 Blue Boxes ( $\square$ ) correspond to the contact of the traced granule with the neighbouring granule.

290 were observed with neighbouring granules (highlighted as blue boxes on the pictures). This  
 291 analysis was carried out to analyze ten different granules, for which we found coordination  
 292 numbers varying from 5 (min) to 8 (max).

293 Therefore, with  $n = (5,8)$  and a Poisson's ratio  $\nu = 0.5$ , values obtained for the particle  
 294 modulus were between  $G_p \approx 5300$  Pa and  $G_p \approx 3300$  Pa.

295 However, as seen in the confocal images, the particles are far from being spherical and  
 296 have hair-like protrusions on the surface. This suggests that friction might be present in the  
 297 system, which is coherent with the measure of a finite shear modulus at low volume fraction,  
 298 the hallmark of the system above random loose packing concentration. Assuming a fully  
 299 frictional case,  $G_p \approx G_{suspension}$  at  $\phi$  around 1, and we obtain  $G_p \approx 550$  Pa.

300 *3.2. Estimation of particle bulk modulus*

301 To estimate the starch granule bulk modulus, we used osmotic compression experiments  
 302 as previously done by de Aguiar et al. (2017) on model microgels. In general terms, the  
 303 isotropic compressibility of material of volume  $V$  under a pressure  $P$  is measured by its bulk  
 304 elastic modulus  $K = -V \frac{dP}{dV}$ . In this study, we do not measure directly the volume of the  
 305 sample, but instead, we determined  $\phi$ , which is directly proportional to the sample volume  
 306 through the relation  $\phi = n_p V_d / V$ , where  $n_p$  is the particle's number in the sample,  $V_d$  is the  
 307 average volume of a fully swollen starch granule in the diluted state, and  $V$  the volume of  
 308 the entire suspension. The bulk modulus of a gelatinized starch paste, compressed under an  
 309 osmotic pressure  $\pi$ , can then be written as  $K = -(1/\phi) \frac{d\pi}{d(1/\phi)}$ , or in a more simple way

$$K = \phi \frac{d\pi_{in}}{d\phi} \quad (6)$$

310 where  $\pi$ ,  $\phi$  are the applied osmotic pressure and the starch particle volume fraction in the  
 311 suspension respectively. In our experiments, the osmotic pressure is directly linked to the  
 312 PEG content in the water bath, so that osmotic pressures ranging from about 18 kPa to  
 313 about 19 kPa were experimentally reached (Table 2)

PEG conc [wt %]	Osmotic pressure [kPa]	Volume fraction( $\phi$ ) [%]
1	1.8	77
1.5	3.4	99
2	5.4	120
2.5	8.0	139
3	11.0	145
3.5	14.7	158
4	18.9	169

Table 2: Equilibrium osmotic pressure and volume fractions

314 Using equation 6, the estimates for bulk modulus at different volume fraction are shown  
 315 in figure 3. Consistently with Nikolov et al. (2020) a linear relationship between suspension  
 316 bulk modulus and volume fraction is obtained. The linear trend also agrees well with  
 317 the experimental results of Liétor-Santos et al. (2011) for microgel particles comprising  
 318 vinyl pyridine and divinyl benzene. Nikolov et al. (2020) showed that suspension bulk



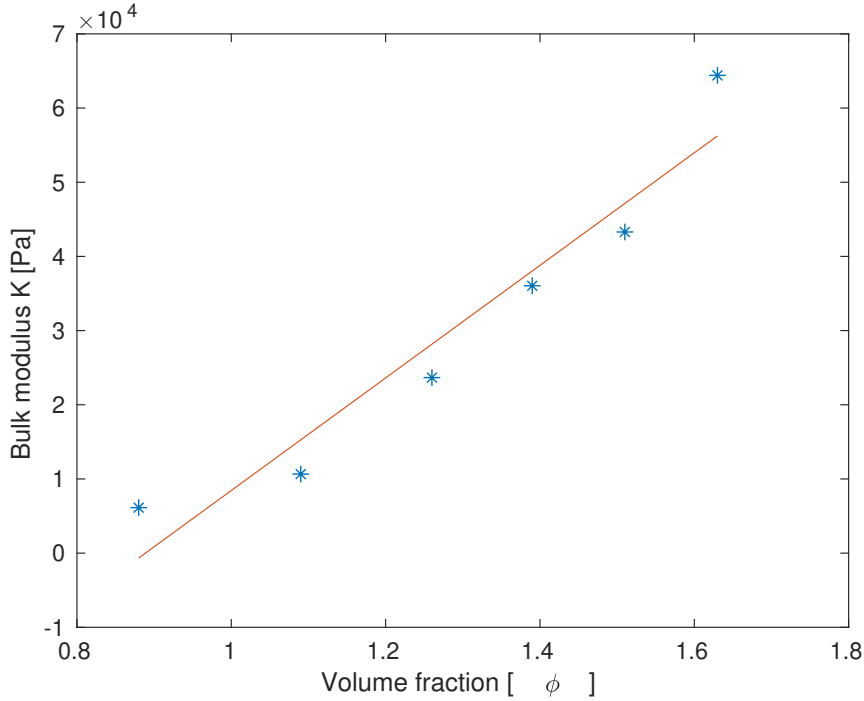


Figure 3: Suspension bulk modulus as function of volume fraction. Asterisks[\*] correspond to experimental data.

319 modulus at  $\phi = 1$  is roughly equal to  $0.8 \times$  particle bulk modulus, and that the ratio of the  
 320 suspension bulk modulus to the particle bulk modulus is independent of volume fraction for  
 321  $\phi > 1$ . From the linear fit in figure 3, it appears that the bulk modulus of the suspension  
 322 is about 8.4 kPa at  $\phi = 1$ . Therefore, an estimate for our starch particle bulk modulus  
 323 is  $K_{particle} \approx 10.5$  kPa. Using this estimate for bulk modulus and shear modulus of the  
 324 suspension at  $\phi = 1$ , we obtain a Poisson's ratio of 0.47, which is close to the maximum  
 325 value of 0.5. By contrast, a Poisson's ratio of 0.33 is obtained if it is calculated using the  
 326 friction-less spherical particle assumption. Poisson's ratio for hydrogels reported in literature  
 327 ranged from 0.38 to 0.5 (Mohapatra et al., 2017; Boon and Schurtenberger, 2017). This  
 328 methodology to characterize the modulus of particles is complementary to the techniques  
 329 such as nano-indentation, AFM, etc (Kaufman et al., 2017; Aufderhorst-Roberts et al., 2018).  
 330 Such existing alternative techniques are not straightforward to apply to measure a particle  
 331 averaged modulus for such a complex system of soft particles with a very high degree of

332 variability in terms of size and shapes.

333 *3.3. Suspension material properties with temperature*

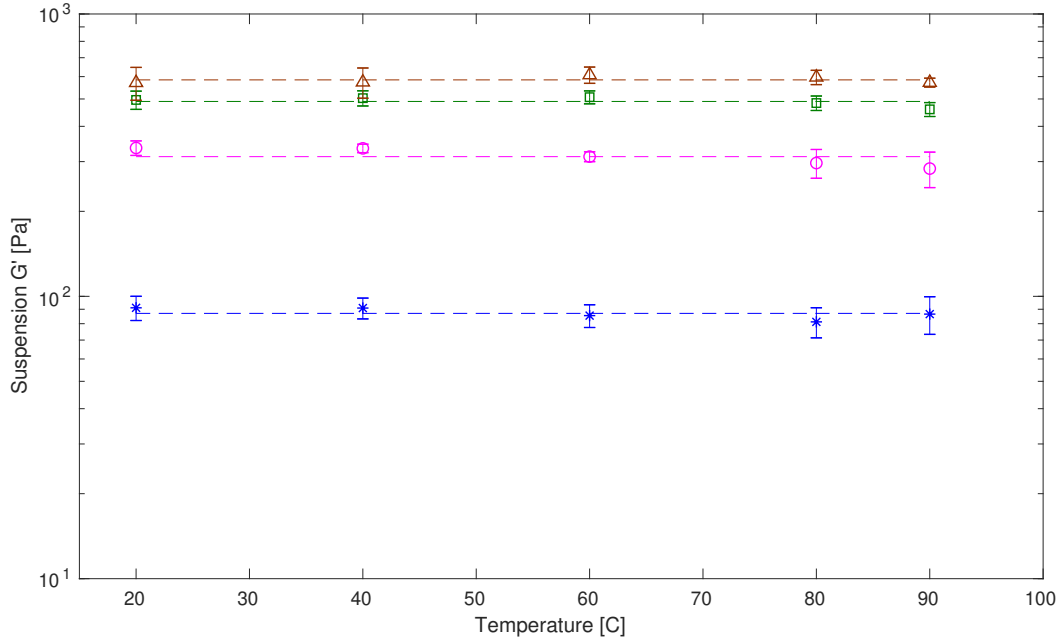


Figure 4: Storage modulus at different temperatures. Asterisks[\*], circles[○], boxes[□] and triangles[△] correspond to volume fractions  $\phi$  of 0.42, 0.63, 0.83 and 1.03 respectively. Error bars correspond to one standard deviation. The dashed line is the mean value of all the measurements across temperatures.

334 The storage modulus of the suspension was measured at five different temperatures for  
335 four different volume fractions. No significant dependence of shear modulus with temper-  
336 ature was observed in the range of temperatures tested. In figure 4 the dotted line is the  
337 mean of the measurements of storage moduli at all temperatures for a given volume fraction.  
338 These dotted lines fall within the error bars for all volume fractions except for  $\phi = 0.63$  at  
339 40 °C. Thus, we conclude that the starch granule material properties are independent of  
340 the temperature for the tested range of 20 °C to 90 °C. Such temperature independence of  
341 hydrogels is also observed by Jing et al. (2021) for polyvinyl alcohol (PVA), carrageenan  
342 and calcium-chloride based particles as long as there is no phase change such as melting.

### 343 3.4. Conclusion

344 This study focused on the rheological properties of fully gelatinized chemically modi-  
345 fied waxy maize starch. We characterized suspension shear modulus and suspension bulk  
346 modulus at different particles volume fractions, which was reached thanks to three different  
347 and independent techniques: centrifugation of a diluted suspension, osmotic compression  
348 of a diluted suspension, and controlled swelling of the granules with a limited amount of  
349 water. These different techniques allowed to reach a large range of volume fractions but also  
350 gave coherent results showing the results are not technique-dependant. The shear and bulk  
351 moduli were determined by rheometry and osmotic compression, respectively. From these  
352 macroscopic measurements, we estimated the mechanical properties of an “averaged” swollen  
353 granule. We first discussed the equation previously used by Evans and Lips (1990), which  
354 can be used to estimate the particle shear modulus from the suspension shear modulus, and  
355 required an estimate of the average number of neighbouring granules. This was roughly  
356 estimated manually using the layered scans of confocal microscopy. Besides Evans and Lips  
357 (1990) equation is only valid for perfectly spherical friction-less spheres, which is rarely the  
358 case in naturally occurring systems such as starch suspensions, this approach could give an  
359 upper bound for the particle shear modulus which was estimated to be around 4400 Pa for  
360 this starch. For the lower bound, we considered frictional interactions so that the particle  
361 shear modulus is nearly identical to the suspension shear modulus at a volume fraction close  
362 to 1. From this assumption, an estimate of particle modulus of 550 Pa was obtained. It  
363 seems reasonable, notably in view of the ‘roughness’ of the observed granules to consider  
364 rather the second hypothesis. Therefore, assuming frictional interactions, the bulk modulus  
365 of the particle was estimated to be around 10.5 kPa. Interestingly, the suspension shear  
366 modulus, measured at different volume fractions, were found to be independent of temper-  
367 ature, which strongly suggests that starch granules mechanical properties are temperature  
368 independent in the range of temperature investigated here. Finally, in a first approach, for  
369 this kind of starch, in a fully swollen state, Young’s modulus and Poisson’s ratio of the  
370 granules are approximately 1.8 kPa and 0.47 respectively. These estimates could find use in  
371 research using modelling and simulation techniques such as DEM and CFD-DEM which in

372 turn help in designing process equipment, process intensification, optimization and design-  
373 ing model-based process control. This methodology can be applied to estimate properties of  
374 similar microgel systems and of different grades of chemically modified waxy maize starches.

#### 375 4. Acknowledgments

376 This research has been carried out with funding from European Union as part of EU  
377 RESEARCH FRAMEWORK PROGRAMME: H2020 / Marie Skłodowska-Curie Actions  
378 ITN MATHEGRAM [813202].

#### 379 References

- 380 A. R. Abate, L. Han, L. Jin, Z. Suo, and D. A. Weitz. Measuring the elastic modulus of microgels using  
381 microdrops. *Soft Matter*, 8(39):10032–10035, 2012.
- 382 N. Abdulmola, M. Hember, R. Richardson, and E. Morris. Effect of xanthan on the small-deformation  
383 rheology of crosslinked and uncrosslinked waxy maize starch. *Carbohydrate Polymers*, 31(1-2):65–78,  
384 1996.
- 385 A. Aufderhorst-Roberts, D. Baker, R. J. Foster, O. Cayre, J. Mattsson, and S. D. Connell. Nanoscale  
386 mechanics of microgel particles. *Nanoscale*, 10(34):16050–16061, 2018.
- 387 G. Batchelor. The effect of brownian motion on the bulk stress in a suspension of spherical particles. *Journal*  
388 *of Fluid Mechanics*, 83(1):97–117, 1977.
- 389 N. Boon and P. Schurtenberger. Swelling of micro-hydrogels with a crosslinker gradient. *Physical Chemistry*  
390 *Chemical Physics*, 19(35):23740–23746, 2017.
- 391 G. Chen, O. H. Campanella, and S. Purkayastha. A dynamic model of crosslinked corn starch granules  
392 swelling during thermal processing. *Journal of Food Engineering*, 81(2):500–507, 2007.
- 393 M. Cloitre, R. Borrega, and L. Leibler. Rheological aging and rejuvenation in microgel pastes. *Physical*  
394 *Review Letters*, 85(22):4819, 2000.
- 395 J. Cohen, R. Podgornik, P. L. Hansen, and V. Parsegian. A phenomenological one-parameter equation of  
396 state for osmotic pressures of peg and other neutral flexible polymers in good solvents. *The Journal of*  
397 *Physical Chemistry B*, 113(12):3709–3714, 2009.
- 398 I. B. de Aguiar, T. Van de Laar, M. Meireles, A. Bouchoux, J. Sprakel, and K. Schroën. Deswelling and  
399 deformation of microgels in concentrated packings. *Scientific Reports*, 7(1):1–11, 2017.
- 400 I. B. de Aguiar, K. Schroën, M. Meireles, and A. Bouchoux. Compressive resistance of granular-scale  
401 microgels: From loose to dense packing. *Colloids and Surfaces A: Physicochemical and Engineering*  
402 *Aspects*, 553:406–416, 2018.

403 F. Deslandes, A. Plana-Fattori, G. Almeida, G. Moulin, C. Doursat, and D. Flick. Estimation of individual  
404 starch granule swelling under hydro-thermal treatment. *Food Structure*, 22:100125, 2019.

405 A. Di Renzo and F. P. Di Maio. An improved integral non-linear model for the contact of particles in distinct  
406 element simulations. *Chemical engineering science*, 60(5):1303–1312, 2005.

407 K. Dong, R. Yang, R. Zou, and A. Yu. Role of interparticle forces in the formation of random loose packing.  
408 *Physical review letters*, 96(14):145505, 2006.

409 A. Einstein. *Eine neue bestimmung der moleküldimensionen*. PhD thesis, ETH Zurich, 1905.

410 I. Evans and A. Lips. Viscoelasticity of gelatinized starch dispersions. *Journal of Texture Studies*, 23(1):  
411 69–86, 1992.

412 I. D. Evans and A. Lips. Concentration dependence of the linear elastic behaviour of model microgel  
413 dispersions. *Journal of the Chemical Society, Faraday Transactions*, 86(20):3413–3417, 1990.

414 R. S. Farr and R. D. Groot. Close packing density of polydisperse hard spheres. *The Journal of chemical  
415 physics*, 131(24):244104, 2009.

416 Y. He, Z. Wang, T. Evans, A. Yu, and R. Yang. Dem study of the mechanical strength of iron ore compacts.  
417 *International Journal of Mineral Processing*, 142:73–81, 2015.

418 H. Jing, J. Shi, P. Guoab, S. Guan, H. Fu, and W. Cui. Hydrogels based on physically cross-linked network  
419 with high mechanical property and recasting ability. *Colloids and Surfaces A: Physicochemical and  
420 Engineering Aspects*, 611:125805, 2021.

421 G. Kaufman, S. Mukhopadhyay, Y. Rokhlenko, S. Nejati, R. Boltyanskiy, Y. Choo, M. Loewenberg, and  
422 C. O. Osuji. Highly stiff yet elastic microcapsules incorporating cellulose nanofibrils. *Soft Matter*, 13(15):  
423 2733–2737, 2017.

424 J. E. Lane, P. T. Metzger, and R. A. Wilkinson. A review of discrete element method (dem) particle shapes  
425 and size distributions for lunar soil. *NASA STI*, 2010.

426 J. Li, M. Turesson, C. A. Haglund, B. Cabane, and M. Skepö. Equation of state of peg/peo in good solvent.  
427 comparison between a one-parameter eos and experiments. *Polymer*, 80:205–213, 2015.

428 J. J. Liétor-Santos, B. Sierra-Martín, and A. Fernández-Nieves. Bulk and shear moduli of compressed  
429 microgel suspensions. *Physical Review E*, 84(6):060402, 2011.

430 J. Mattsson, H. M. Wyss, A. Fernandez-Nieves, K. Miyazaki, Z. Hu, D. R. Reichman, and D. A. Weitz. Soft  
431 colloids make strong glasses. *Nature*, 462(7269):83–86, 2009.

432 P. Menut, S. Seiffert, J. Sprakel, and D. A. Weitz. Does size matter? elasticity of compressed suspensions  
433 of colloidal-and granular-scale microgels. *Soft Matter*, 8(1):156–164, 2012.

434 H. Mohapatra, T. M. Kruger, T. I. Lansakara, A. V. Tivanski, and L. L. Stevens. Core and surface microgel  
435 mechanics are differentially sensitive to alternative crosslinking concentrations. *Soft matter*, 13(34):5684–  
436 5695, 2017.

437 H. Nawaz, R. Waheed, M. Nawaz, and D. Shahwar. Physical and chemical modifications in starch structure  
438 and reactivity. *Chemical properties of starch*, page 13, 2020.

439 S. V. Nikolov, A. Fernandez-Nieves, and A. Alexeev. Behavior and mechanics of dense microgel suspensions.  
440 *Proceedings of the National Academy of Sciences*, 117(44):27096–27103, 2020.

441 L. Orefice and J. G. Khinast. A novel framework for a rational, fully-automatised calibration routine for  
442 dem models of cohesive powders. *Powder Technology*, 361:687–703, 2020.

443 A. Palanisamy, F. Deslandes, M. Ramaioli, P. Menut, A. Plana-Fattori, and D. Flick. Kinetic modelling of  
444 individual starch granules swelling. *Food Structure*, page 100150, 2020.

445 D. S. Preece, R. P. Jensen, E. D. Perkins, J. R. Williams, et al. Sand production modeling using superquadric  
446 discrete elements and coupling of fluid flow and particle motion. In *Vail Rocks 1999, The 37th US*  
447 *Symposium on Rock Mechanics (USRMS)*. American Rock Mechanics Association, 1999.

448 W. S. Ratnayake and D. S. Jackson. Starch gelatinization. *Advances in Food and Nutrition Research*, 55:  
449 221–268, 2008.

450 S. Renzetti, I. A. van den Hoek, and R. G. van der Sman. Mechanisms controlling wheat starch gelatinization  
451 and pasting behaviour in presence of sugars and sugar replacers: Role of hydrogen bonding and plasticizer  
452 molar volume. *Food Hydrocolloids*, 119:106880, 2021.

453 Reportlinker.com. Global starch industry. *GLOBE NEWSWIRE, New York*, 2020.

454 A. Rodriguez-Hernandez, S. Durand, C. Garnier, A. Tecante, and J. L. Doublier. Rheology-structure prop-  
455 erties of waxy maize starch–gellan mixtures. *Food Hydrocolloids*, 20(8):1223–1230, 2006.

456 J. R. Seth, M. Cloitre, and R. T. Bonnecaze. Elastic properties of soft particle pastes. *Journal of rheology*,  
457 50(3):353–376, 2006.

458 H. M. Shewan and J. R. Stokes. Analytically predicting the viscosity of hard sphere suspensions from the  
459 particle size distribution. *Journal of Non-Newtonian Fluid Mechanics*, 222:72–81, 2015a.

460 H. M. Shewan and J. R. Stokes. Viscosity of soft spherical micro-hydrogel suspensions. *Journal of colloid*  
461 *and interface science*, 442:75–81, 2015b.

462 H. M. Shewan, G. E. Yakubov, M. R. Bonilla, and J. R. Stokes. Viscoelasticity of non-colloidal hydrogel  
463 particle suspensions at the liquid–solid transition. *Soft Matter*, 17(19):5073–5083, 2021.

464 L. E. Silbert. Jamming of frictional spheres and random loose packing. *Soft Matter*, 6(13):2918–2924, 2010.

465 K. van der Vaart, Y. Rahmani, R. Zargar, Z. Hu, D. Bonn, and P. Schall. Rheology of concentrated soft  
466 and hard-sphere suspensions. *Journal of Rheology*, 57(4):1195–1209, 2013.

467 M. van Hecke. Jamming of soft particles: geometry, mechanics, scaling and isostaticity. *Journal of Physics:*  
468 *Condensed Matter*, 22(3):033101, 2009.

469 M. M. Villone and H. A. Stone. Rotating tensiometer for the measurement of the elastic modulus of  
470 deformable particles. *Physical Review Fluids*, 5(8):083606, 2020.

471 M. M. Villone, J. K. Nunes, Y. Li, H. A. Stone, and P. L. Maffettone. Design of a microfluidic device for  
472 the measurement of the elastic modulus of deformable particles. *Soft matter*, 15(5):880–889, 2019.

473 Z. Yan, S. K. Wilkinson, E. H. Stitt, and M. Marigo. Investigating mixing and segregation using discrete  
474 element modelling (dem) in the freeman ft4 rheometer. *International journal of pharmaceutics*, 513(1-2):  
475 38–48, 2016.